Quantitative Assessment of Image Quality in 64-slice-computed Tomography of Coronary Arteries in Subjects Undergoing Screening for Coronary Artery Disease

Li-Hwa Yang,[1] Ding-Kwo Wu,[1,2] Chiao-Yun Chen,[1,2] Gin-Chung Liu,[1,2] Tsyh-Jyi Hsieh,[1,2] Twei-Shiun Jaw,[1,2] Shu-Yuan Huang,[1] Chien-Chung Lin,[1] and Jui-Sheng Hsu[3,4]

[1]Department of Medical Imaging, Kaohsiung Medical University Hospital; [2]Department of Radiology, Faculty of Medicine, [3]Graduate Institute of Medicine College of Medicine, and [4]Department of Medical Imaging, Kaohsiung Municipal Hsiao-Kang Hospital, Kaohsiung Medical University, Kaohsiung, Taiwan.

Accurate and consistent visualization of the entire coronary system with high-grade imaging quality is crucial for routine applications of multi-detector-computed tomography (MDCT) coronary angiography. To determine the imaging quality of 64-slice-MDCT coronary angiography, we respectively explored the quantitative parameters of imaging quality in 105 consecutive subjects (71 men, 34 women; aged 58.66 ± 10.62 years) who underwent 64-slice-MDCT coronary angiography to screen for coronary disease. The interobserver agreement for semi-quantitative image quality, visible length, signal-to-noise ratio (SNR) and contrast-to-noise ratio (CNR) of the coronary arteries was good. The SNR and CNR of the proximal segments of the coronary arteries were superior to that of the distal segments of coronary arteries ($p < 0.001$). The visible length of the stenosed right coronary artery was significantly shorter than that of the non-stenosed right coronary artery ($p = 0.03$). The SNR and CNR of the stenosed and non-stenosed coronary arteries revealed no significant difference ($p > 0.05$). Body weight and body mass index were inversely related to the SNR and CNR of the aorta ($p < 0.001$). In conclusion, 64-slice-MDCT coronary angiography can provide excellent imaging quality of coronary arteries in subjects undergoing screening for coronary disease, although the SNR and CNR were relatively low at the distal segments of coronary arteries.

Key Words: computed tomography, coronary artery
(*Kaohsiung J Med Sci* 2010;26:21–9)

Coronary artery disease (CAD) is a major cause of morbidity and mortality worldwide. Conventional invasive coronary angiography is currently the clinical gold standard for the detection of CAD. However, the risk of potentially serious adverse complications and the associated cost have prompted intensive searches for noninvasive alternatives. Advances in multi-detector-computed tomography (MDCT) have improved imaging quality and simplified the implementation of contrast-enhanced MDCT in noninvasive cardiovascular imaging programs [1–5]. The improved imaging quality has increased the accuracy of MDCT imaging for the diagnosis of coronary artery stenosis when compared with conventional invasive coronary angiography. A recent meta-analysis [6]

Received: Aug 20, 2009 Accepted: Sep 9, 2009
Address correspondence and reprint requests to: Dr Jui-Sheng Hsu, Department of Medical Imaging, Kaohsiung Municipal Hsiao-Kang Hospital, 482 San-Ming Road, Hsiao-Kang District, 812 Kaohsiung City, Taiwan.
E-mail: e3124@ms16.hinet.net

showed a clear increase in diagnostic accuracy as technology improved from 4-slice-MDCT to 16-slice- and 64-slice-MDCT, with a pooled sensitivity of 95% and specificity of 93% for 64-slice-MDCT on a per-vessel basis. On a per-patient analysis, the pooled sensitivity for 64-slice-MDCT was 99% and the specificity was 93%. Nevertheless, 29% of the coronary arteries could not be evaluated because of insufficient imaging quality with 4-slice-MDCT, 22–29% with 16-slice-MDCT, and 3–11% with 64-slice-MDCT [7–15]. High heart rate and greater body mass index (BMI) have been implicated as the major factors that degrade the imaging quality of MDCT coronary angiography [7,12,16–19]. Stenosis of coronary arteries might impede the enhancement of the post-stenosed coronary arteries. To our knowledge, the influence of stenosed coronary arteries on imaging quality of MDCT coronary angiography has not been reported. Accurate and consistent visualization of the entire coronary system with high-grade imaging quality is crucial for routine applications of MDCT coronary angiography. The purpose of our study was to quantitatively assess the imaging quality of coronary arteries in subjects undergoing 64-slice-MDCT coronary angiography to screen for CAD.

Subjects and Methods

Study population

This study was approved by our institutional human research committee. We retrospectively studied 105 consecutive patients (74 men and 34 women) referred for CAD screening between January 1 and October 31, 2007. Standard exclusion criteria for contrast-enhanced MDCT coronary angiography were applied, and included previous allergic reaction to iodinated contrast, atrial fibrillation or other arrhythmias, or renal disease with serum creatinine level > 1.5 mg/dL.

MDCT coronary protocol

All patients were assessed 60–90 minutes before their scheduled scan appointment to determine if they were clinically and hemodynamically stable. Heart rate and blood pressure were recorded. If the heart rate exceeded 65 beats per minute with a systolic blood pressure above 100 mmHg, and the patient was without contraindications for β-blockers, an oral dose of 5 mg of bisoprolol (Concor, Merck, Darmstadt, Germany) was administered to reduce the heart rate to improve image quality. In addition, in the absence of contraindications, patients received a sublingual dose of nitrate (0.6 mg of nitroglycerin; Nitrostat, Pfizer, USA) to dilate the coronary arteries.

MDCT scans were performed on a 64-slice-MDCT (Brilliance 64; Philips Medical Systems, Haifa, Israel). Patients were examined in the supine position, and all image acquisitions were performed during an inspiratory breath-hold. The breath-hold time was between 10–20 seconds, depending on the scanning volume. A bolus of 60–80 mL of Iohexol (Omnipaque 350; GE Healthcare, Cork, Ireland) was injected into an antecubital vein at a flow rate of 4–5 mL/s, followed by a 50-mL saline chasing bolus. The start delay was defined by bolus tracking in the ascending aorta and the scan was automatically started 10 seconds after reaching the threshold (150 Hounsfield units). Scanning was performed from the tracheal carina to the diaphragm using the following parameters: X-ray tube potential = 120 kV, effective tube current = 800 mAs, detector collimation = 64 × 0.625 mm, rotation time = 420 ms, and pitch = 0.2.

For image reconstruction, we processed the source images on a separate workstation (Brilliance 2.0; Philips Medical Systems). We used retrospective electrocardiographic gating for optimal heart phase selection. The images were reconstructed and synchronized to electrocardiography during the late diastole phase at 70–80% of the RR interval. Slices with a thickness of 1 mm (increment = 0.6 mm) and a medium soft-tissue reconstruction kernel were used to evaluate the coronary arteries. Evaluation of vessel visibility was performed on each edited data set by two experienced radiologists (Dr D.K. Wu and Dr C.Y. Chen) to select the best phase for further vessel segment analysis using a combination of axial, multi-planar reformation and maximum intensity projection views on an image post-processing workstation (Brilliance 2.0; Philips Medical Systems).

MDCT image analysis

Two experienced radiologists, acting independently, performed a semi-quantitative assessment of the overall image quality using a four-point scale, as reported previously [20], where 4 = excellent, no artifact; 3 = good, mild artifact; 2 = acceptable, moderate artifact present but images still interpretable; and

1 = unmeasurable, severe artifact renders interpretation not possible. For any disagreement in data analysis between the two observers, consensus agreement was achieved. Stenosis of the coronary artery was defined as at least one segment of the coronary artery with a ≥50% reduction in diameter based on cross-sectional image analysis [2].

The overall visible length of each coronary artery was determined by manually measuring the centerline length from the ostium to the most distal point at which the enhanced vessel lumen was still clearly visible in the curved multi-planar reformatted images by two independent, experienced observers (Dr L.H. Yang and Dr T.J. Hsieh). We measured the length of the left main coronary artery (LM), left anterior descending coronary artery (LAD), left circumflex coronary artery (LCX) and right coronary artery (RCA). The length of the LCX was defined as the length of the entire LCX or the length of the proximal LCX and the first obtuse marginal branch, if this branch had a larger diameter [12].

To determine the signal-to-noise ratio (SNR) and the contrast-to-noise ratio (CNR), a region-of-interest (ROI) cursor (3–4 mm^2) was placed within the contrast-enhanced lumen of the coronary artery and the connective tissue adjacent to the vessel, and the signal intensity (SI; i.e. CT attenuation) was recorded by the two experienced observers. The ROIs were positioned by carefully avoiding calcifications, plaques, and vessel walls. The mean SI of both observations was calculated for further evaluation. We measured nine locations: LM, proximal LAD, distal LAD (distal portion), proximal first diagonal branch, proximal LCX, distal LCX (distal portion), first obtuse marginal branch (proximal part), proximal RCA, and distal RCA (distal portion of the posterior descending coronary artery). Image noise was defined as the standard deviation (SD) of SI in a ROI cursor (1 cm^2) placed in the aortic root at the level of the origin of the LM. SNR, CNR, SNR of the proximal–distal difference and CNR of the proximal–distal difference were calculated using the following equations:

$$\text{SNR} = \text{SI}_{\text{lumen}} / \text{imaging noise};$$
$$\text{CNR} = (\text{SI}_{\text{lumen}} - \text{SI}_{\text{connective tissue}}) / \text{imaging noise};$$
$$\text{SNR of the proximal–distal difference} = (\text{SNR}_{\text{proximal}} - \text{SNR}_{\text{distal}});$$
$$\text{CNR of the proximal–distal difference} = (\text{CNR}_{\text{proximal}} - \text{CNR}_{\text{distal}});$$

where SI_{lumen} is the mean SI of the coronary artery, $SI_{connective\ tissue}$ is the mean SI of the connective tissue adjacent to the vessel, image noise is the SD of SI in the aortic root, $SNR_{proximal}$ is the SNR of the proximal segment of coronary artery, SNR_{distal} is the SNR of the distal segment of coronary artery, $CNR_{proximal}$ is the CNR of the proximal segment of coronary artery, and CNR_{distal} is the CNR of the distal segment of coronary artery.

Statistical analysis

All data are expressed as means ± SD. The results are reported as the mean of the measurements by two observers. Wilcoxon signed-rank test and κ statistics were applied for interobserver agreement of semi-quantitatively imaging quality assessment. Pearson's correlation coefficient and Student's paired *t* test were used to determine the interobserver agreement for the visible length, SNR and CNR of the coronary arteries. Linear regression analysis was preformed to plot the effects of heart rate on semi-quantitative imaging quality. Differences among arteries (SNR and CNR) were examined using one-way analysis of variance. Differences between individual pairs were then analyzed using Bonferroni's multiple comparison test. Student's *t* test was used to determine the difference between the stenosed and non-stenosed coronary arteries. Linear regression analysis was performed to explore the influence of heart rate, body weight, BMI and SNR of the aortic root on the CNR of the aortic root and coronary arteries.

RESULTS

Patient characteristics

The mean age of the 105 subjects in the study was 58.66 ± 10.62 years (range, 30–85 years). The mean heart rate during the scan was 59 ± 8 beats/min. The mean body weight was 68.36 ± 10.76 kg and mean BMI was 24.98 ± 3.13 kg/m^2. Results showed stenosis at the RCA in 26 subjects, LAD in 39 subjects and LCX in 16 subjects. Stenosis of the RCA (n = 5), LAD (n = 6) and LCX (n = 5) was confirmed by conventional coronary angiography in 11 subjects.

The semi-quantitative imaging quality for each coronary artery is summarized in Table 1. In 105 subjects, a total of 360 vessels were evaluated. The overall interobserver agreement for the semi-quantitative

imaging quality rating was good (κ = 0.67, $p = 0.56$). All coronary segments were of diagnostic imaging quality (score 2–4; Figure 1), with 551 segments (87.5%) were rated to have excellent imaging quality (score = 4), 49 (8.8%) had mild artifacts (score = 3) and 30 (5.8%) had moderate artifacts (score = 2). No coronary segments were rated as non-diagnostic coronary segments (score = 1).

The interobserver agreement for the visible length of the coronary arteries was good. The visible length (and correlation coefficients) of the coronary arteries was: LM, 10.2 ± 4.6 mm ($r = 0.99$, $p = 0.77$); LAD, 140.6 ± 26.2 mm ($r = 0.96$, $p = 0.26$); LCX, 94.3 ± 30.4 mm ($r = 0.99$, $p = 0.32$); and RCA, 158.2 ± 34.7 mm ($r = 0.78$, $p = 0.12$). The visible length of the stenosed RCA was significantly shorter than that of the non-stenosed RCA (145.9 ± 31.1 *vs*. 162.2 ± 35.1 mm, $p = 0.03$). Assessment of the visible length of the coronary arteries revealed no significant difference between stenosed and non-stenosed groups of LAD (135.3 ± 24.0 mm *vs*. 143.7 ± 27.1 mm, $p = 0.10$) and LCX (104.8 ± 22.7 mm *vs*. 92.4 ± 31.4 mm, $p = 0.07$).

Table 1. Semi-quantitative scores of image quality and interobserver agreement for the coronary arteries of 105 subjects*

Variable	Semi-quantitative imaging quality		
	Mean ± SD	κ coefficient	*p*
LM	3.99 ± 0.10	0.99	0.99
LAD	3.74 ± 0.56	0.59	0.58
D1	3.90 ± 0.37	0.79	0.58
LCX	3.80 ± 0.48	0.61	0.34
OM1	3.72 ± 0.63	0.92	0.99
RCA	3.75 ± 0.54	0.78	0.42
Total coronary arteries	3.82 ± 0.49	0.67	0.56

*The interobserver agreement for semi-quantitative rating of image quality of coronary arteries was good. SD = standard deviation; LM = left main coronary artery; LAD = left anterior descending coronary artery; D1 = first diagonal branch; LCX = left circumflex coronary artery; OM1 = first obtuse marginal branch; RCA = right coronary artery.

The interobserver agreement for SNR and CNR of each coronary artery showed excellent agreement (Table 2). No significant differences in SNR and CNR were observed among LM and the proximal segments of the RCA, LAD and LCX (SNR, $p = 0.25$; CNR, $p = 0.44$). The SNR of the distal segments of the RCA and LCX was superior to that of the distal segments of the LAD ($p < 0.001$). No significant difference was observed for the CNR among the distal segments of the RCA, LAD and LCX ($p = 0.24$). The SNR of the proximal segments of the coronary arteries was superior to that of the distal fragments of coronary arteries in the RCA, LAD and LCX ($p < 0.001$). The CNR of the proximal segments of the coronary arteries was higher than that of the distal fragments of the coronary arteries in the RCA, LAD and LCX ($p < 0.001$). The SNR and CNR were significantly higher in the proximal LAD than in the proximal first diagonal branch of the LAD ($p < 0.001$). The SNR and CNR of the proximal LCX were higher than those of the first obtuse marginal branch of LCX ($p < 0.001$).

The SNR and CNR of the stenosed and non-stenosed coronary arteries are summarized in Table 3. The SNR and CNR showed no significant difference

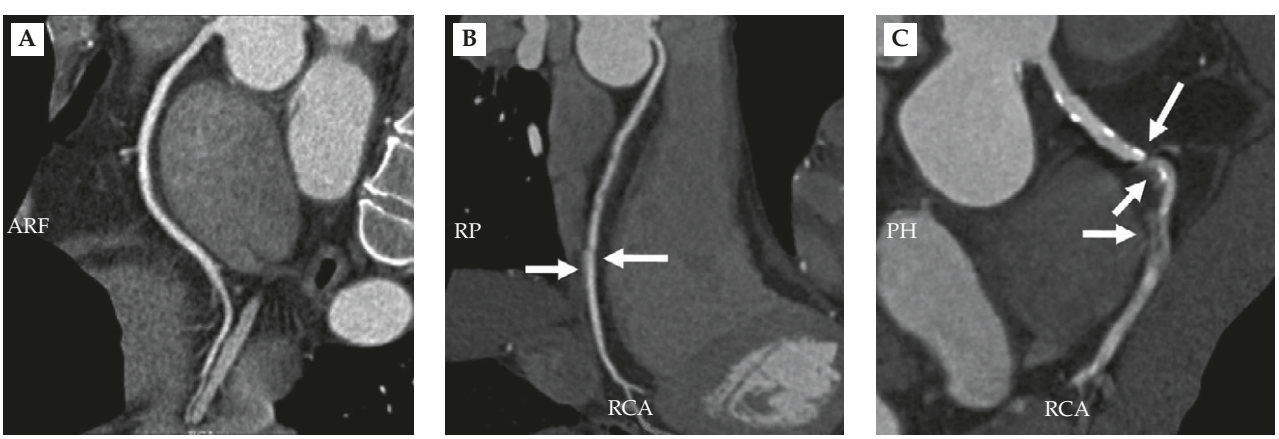

Figure 1. *Curved multiplanar reformatted images of the right coronary arteries (A) for an excellent image with no artifacts; (B) a good image with mild motion artifacts and step artifacts (arrows); and (C) an acceptable image with moderate motion artifacts and step artifacts (arrows). RCA = right coronary artery.*

Table 2. Mean signal-to-noise ratio, contrast-to-noise ratio and interobserver agreement in the coronary arteries of 105 subjects*

Variable	Signal-to-noise ratio			Contrast-to-noise ratio		
	Mean ± SD	*r*	*p*	Mean ± SD	*r*	*p*
Aorta	15.44 ± 4.15	0.90	0.71	18.10 ± 4.36	0.93	0.3
LM	15.31 ± 4.04	0.92	0.11	17.93 ± 4.20	0.91	0.2
Proximal LAD	14.44 ± 3.94	0.93	0.38	17.21 ± 4.15	0.9	0.97
Distal LAD	2.97 ± 1.99	0.98	0.84	6.26 ± 1.63	0.93	0.13
Proximal D1	10.98 ± 3.90	0.97	0.14	14.16 ± 4.29	0.94	0.92
Proximal LCX	14.72 ± 4.06	0.98	0.27	17.74 ± 4.61	0.89	0.65
Distal LCX	4.14 ± 2.31	0.98	0.82	6.22 ± 2.41	0.89	0.3
Proximal OM1	11.45 ± 3.67	0.96	0.36	14.44 ± 4.10	0.93	0.77
Proximal RCA	14.53 ± 4.36	0.95	0.15	17.34 ± 4.62	0.88	0.81
Distal RCA	4.41 ± 2.36	0.99	0.52	6.67 ± 2.25	0.93	0.13

*The interobserver agreement for the signal-to-noise ratio and contrast-to-noise ratio of the coronary arteries was excellent. SD = standard deviation; *r* = Pearson's correlation coefficient; LM = left main coronary artery; LAD = left anterior descending coronary artery; D1 = first diagonal branch; LCX = left circumflex coronary artery; OM1 = first obtuse marginal branch; RCA = right coronary artery.

Table 3. The signal-to-noise ratio and contrast-to-noise ratio of stenosed and non-stenosed coronary arteries*

Variables	Stenosed			Non-stenosed			*p*	
	n	SNR	CNR	*n*	SNR	CNR	SNR	CNR
RCA								
Proximal	26	13.9 ± 3.9	16.7 ± 3.5	79	14.7 ± 4.6	17.5 ± 4.9	0.35	0.34
Distal	26	4.4 ± 2.7	6.6 ± 2.7	79	4.4 ± 2.3	6.7 ± 2.1	0.96	0.88
Difference	26	9.5 ± 3.1	10.1 ± 3.0	79	10.3 ± 4.3	10.9 ± 4.6	0.31	0.34
LAD								
Proximal	39	13.6 ± 3.2	16.3 ± 3.2	66	14.7 ± 4.4	17.5 ± 4.7	0.15	0.14
Distal	39	2.6 ± 1.8	6.2 ± 1.5	66	3.2 ± 2.1	6.3 ± 1.7	0.12	0.62
Difference†	39	11.0 ± 3.2	10.2 ± 2.9	66	11.5 ± 4.3	11.2 ± 4.3	0.51	0.16
LCX								
Proximal	16	13.6 ± 2.9	16.5 ± 3.0	89	14.9 ± 4.2	18.0 ± 4.8	0.14	0.11
Distal	16	3.7 ± 2.3	6.0 ± 2.7	89	4.2 ± 2.4	6.2 ± 2.5	0.49	0.75
Difference†	16	9.9 ± 2.5	10.5 ± 2.6	89	10.8 ± 4.0	11.8 ± 4.4	0.26	0.13

*Data presented as *n* or mean ± standard deviation; †proximal–distal difference of the coronary arteries. SNR = signal-to-noise ratio; CNR = contrast-to-noise ratio; RCA = right coronary artery; LAD = left anterior descending coronary artery; LCX = left circumflex coronary artery.

between the stenosed and non-stenosed groups for the proximal segments, distal segments and the proximal–distal difference of the coronary arteries ($p > 0.05$). The SNR and CNR of the proximal segments of coronary arteries were superior to that of the distal fragments of coronary arteries in both the stenosed and non-stenosed groups ($p < 0.001$).

The SNR of the aorta was proportional to the CNR of the aorta ($p < 0.001$; Figure 2). Body weight and BMI were inversely proportional to the SNR and CNR of the aorta ($p < 0.001$; Figure 2). The SNR and CNR of the aortic root did not significantly affect the visible length of the coronary arteries ($p > 0.05$). Heart rate did not significantly affect semi-quantitative imaging quality, CNR or SNR of the coronary arteries ($p > 0.05$).

Discussion

The study was designed to semi-quantitatively assess the image quality of 64-slice-MDCT coronary angiography in subjects undergoing screening for CAD. We showed that 64-slice-MDCT coronary angiography provided excellent image quality for these subjects. As a result of the technical developments that have improved the spatial resolution through thinner slice

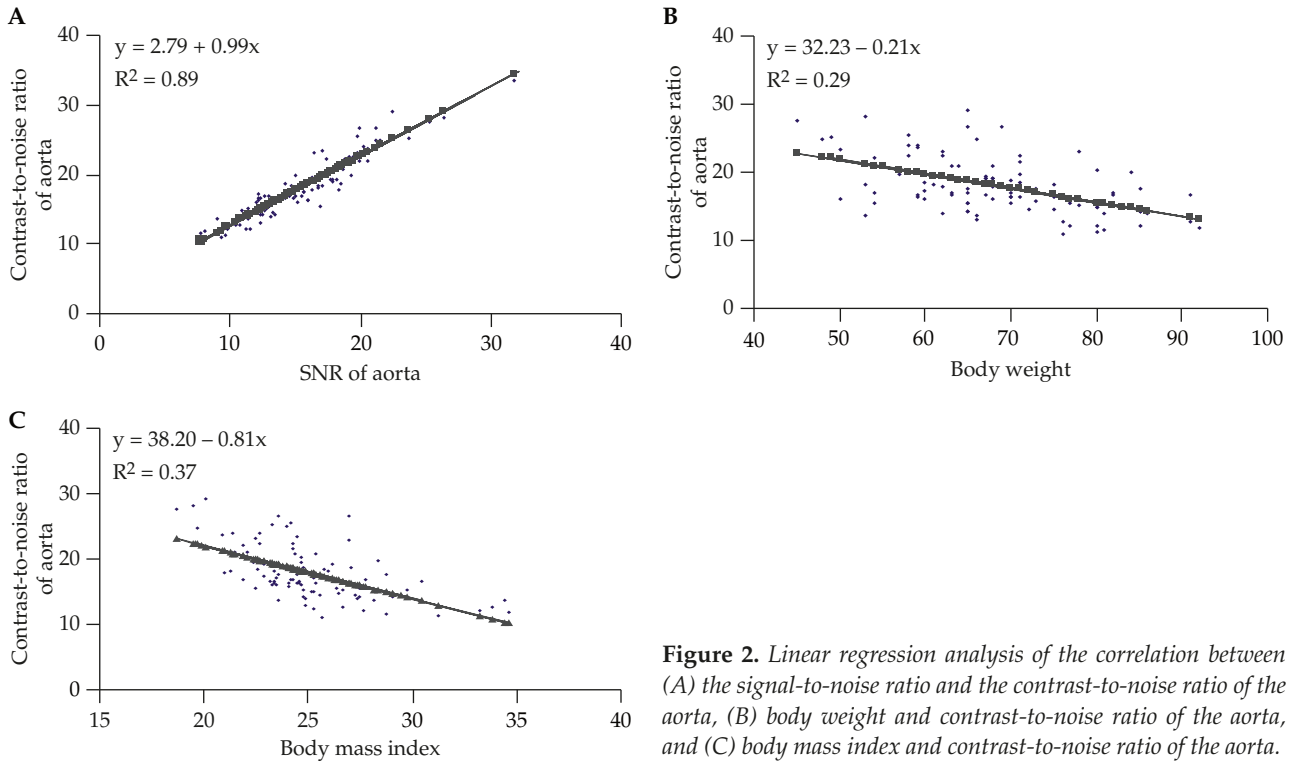

Figure 2. *Linear regression analysis of the correlation between (A) the signal-to-noise ratio and the contrast-to-noise ratio of the aorta, (B) body weight and contrast-to-noise ratio of the aorta, and (C) body mass index and contrast-to-noise ratio of the aorta.*

collimation and increased the temporal resolution through faster gantry rotation, 64-slice-MDCT has become a robust technology for non-invasive coronary imaging [12]. Premedication with β-blockers for subjects with heart rate exceeding 65 beats/min, administration of nitroglycerin, and optimization of the contrast injection protocols further improved the image quality of 64-slice-MDCT coronary angiography.

The mean visible length of the coronary arteries was similar to the previously reported values determined by 16-slice-MDCT and 64-slice-MDCT [12,21]. These results most likely reflect the fact that 64-slice-MDCT scanners provide only stable improvements in spatial resolution, as compared with the 16-slice-MDCT scanner [12]. However, our study showed that the visible length of the stenosed RCA was significantly shorter than that of the non-stenosed RCA. These findings suggest that stenosis of the coronary arteries might reduce the visible length of the post-stenosed coronary arteries.

The best criterion for objectively assessing image quality is the determination of SNR and CNR [22]. We found excellent SNR and CNR in most of the subjects studied. High SNR and CNR were maintained throughout the coronary tree, although the SNR and CNR were lower at the distal segments of the coronary arteries than at the proximal segments of coronary arteries. The ROI measurements of the proximal segment of coronary arteries plus a point at the distal segment provided initial insight into the gradient of contrast enhancement. Although the ROI measurements were difficult and potentially less accurate for small caliber arteries, the 64-slice-MDCT imaging environment yielded excellent interobserver agreement.

Our results indicate that the SNR and CNR of the proximal segments of the coronary arteries were superior to those of the distal fragments of coronary arteries. Our results were different to those in the study by Ferencik et al [12], who showed no significant difference in CNR between the proximal and distal segments of the RCA, although the CNR was significantly higher in the proximal segments of the LAD and LCX than in the distal fragments of the LAD and LCX [12]. In addition, we found no significant difference in the proximal–distal difference of the coronary arteries between the stenosed and non-stenosed coronary arteries. A potentially decreased SNR or CNR of the distal coronary segments might reduce the diagnostic

performance of MDCT coronary angiography. Inadequate contrast administration (e.g. inadequate volume, injection speed or timing), inadequate selection of the field of view or ROI placement for bolus tracking, or inadequate breath-holds can result in low SNR and low CNR, resulting in poorly visualized coronary arteries. Contrast media with higher iodine concentrations provide substantially higher attenuation values in the coronary arteries [23] although the added value of these higher iodine concentration media on diagnostic accuracy in assessing CAD has not yet been established. However, as described by Fleischmann et al [24], arterial enhancement is dependent on the iodine administration rate and injection duration. At a constant iodine load, the injection duration of more concentrated contrast agents is shorter. Although we followed the rule "injection duration equals scanning duration", shorter injection time might reduce image quality because the enhancement is non-uniform over time, with the brightest enhancement occurring out of the imaging acquisition [24]. Faster coronary angiography acquisition using MDCT with 64 or more detectors will possibly benefit from higher concentrations of contrast agents [12].

It is well known that image noise correlates with biometric data such as body weight and BMI [16–18]. Greater body weight and BMI are associated with greater image noise, thus reducing SNR and CNR, and negatively affecting the quality of MDCT coronary angiography. Therefore, our results were in agreement with previous studies.

Heart rate is also a major predictor of MDCT coronary angiography image quality [7,12,19]. Patients with higher heart rates had significantly more motion artifacts. Our results revealed that the heart rate did not significantly influence the semi-quantitative assessment of imaging quality, or SNR or CNR of the coronary arteries. The systematic approach to heart rate control, as performed in this study, was probably one of the major contributors to improved image quality.

Our study has some limitations, which need to be addressed. First, the patient group only included a small number of cases with stenosis of the coronary artery. Second, our study was principally limited by its retrospective nature, which might have introduced selection bias. Third, we only included subjects undergoing screening, which might represent inclusion bias. Fourth, the semi-quantitative rating of image quality may have been biased by subjectivity; however, the high κ coefficient indicated good inter-observer agreement and may argue against such a bias. Fifth, our study lacked direct comparison to previous generations of MDCT scanners in the same patient group. Thus the improved image quality could be partly attributed to different population variables (e.g. patient size and body weight, and heart rate). Sixth, we did not calculate the estimated radiation dose using the exposure parameters provided by the CT scanner. In general, image noise is inversely proportional to the square root of the radiation dose. In other words, reducing the radiation dose may increase image noise and decrease the SNR and CNR. Finally, the systematic approach to heart rate control, as performed in this study, might not be reasonable for routine CT coronary angiography. Faster coronary angiography acquisition using MDCT with 256 or more detectors will benefit from whole heart coverage and sub-second acquisition of the entire cardiac volume. Whole heart coverage might eliminate the "stair-step" artifacts inherent in 64-slice-MDCT, which images sub-volumes of the entire cardiac volume over multiple gantry rotations. Sub-second acquisition of the entire cardiac volume might enable imaging of the contrast bolus at a single time-point to reduce contrast opacification gradients of the coronary arteries.

In conclusion, we have demonstrated that body weight, BMI and the SNR of the aortic root might affect the image quality of 64-slice-MDCT coronary angiography. The 64-slice-MDCT coronary angiography can provide excellent imaging quality of coronary arteries in subjects undergoing screening for coronary disease, although the SNR and CNR were relatively low in the distal segments of coronary arteries. In addition, no significant difference of imaging quality was found between the stenosed and non-stenosed coronary arteries, except that the visible length of the stenosed RCA was shorter than that of the non-stenosed RCA. Overall, 64-slice-MDCT coronary angiography could provide excellent image quality for non-invasive screening of CAD.

Acknowledgments

We are grateful to the Kaohsiung Medical University Hospital, Taiwan, for financial support (KMU-95-5N35).

References

1. Gershlick AH, de Belder M, Chambers J, et al. Role of non-invasive imaging in the management of coronary artery disease: an assessment of likely change over the next 10 years. A report from the British Cardiovascular Society Working Group. *Heart* 2007;93:423–31.
2. Hoe JW, Toh KH. A practical guide to reading CT coronary angiograms—how to avoid mistakes when assessing for coronary stenoses. *Int J Cardiovasc Imaging* 2007;23:617–33.
3. Limkakeng AT, Halpern E, Takakuwa KM. Sixty-four-slice multidetector computed tomography: the future of ED cardiac care. *Am J Emerg Med* 2007;25:450–8.
4. Ramos JJ, Williams M, Synetos A, et al. Clinical utility of cardiac computed tomography. *Am J Med Sci* 2007; 334:350–5.
5. Baur LH. Cardiac imaging at the emergency department is a must! The role of cardiac computed tomography and magnetic resonance imaging in the evaluation of acute chest pain in the emergency department. *Int J Cardiovasc Imaging* 2008;24:343–4.
6. Vanhoenacker PK, Heijenbrok-Kal MH, Van Heste R, et al. Diagnostic performance of multidetector CT angiography for assessment of coronary artery disease: meta-analysis. *Radiology* 2007;244:419–28.
7. Kroft LJ, de Roos A, Geleijns J. Artifacts in ECG-synchronized MDCT coronary angiography. *AJR Am J Roentgenol* 2007;189:581–91.
8. Giesler T, Baum U, Ropers D, et al. Noninvasive visualization of coronary arteries using contrast-enhanced multidetector CT: influence of heart rate on image quality and stenosis detection. *AJR Am J Roentgenol* 2002;179:911–6.
9. Nikolaou K, Knez A, Rist C, et al. Accuracy of 64-MDCT in the diagnosis of ischemic heart disease. *AJR Am J Roentgenol* 2006;187:111–7.
10. Heuschmid M, Kuettner A, Schroeder S, et al. ECG-gated 16-MDCT of the coronary arteries: assessment of image quality and accuracy in detecting stenoses. *AJR Am J Roentgenol* 2005;184:1413–9.
11. Garcia MJ, Lessick J, Hoffmann MH. Accuracy of 16-row multidetector computed tomography for the assessment of coronary artery stenosis. *JAMA* 2006;296:403–11.
12. Ferencik M, Nomura CH, Maurovich-Horvat P, et al. Quantitative parameters of image quality in 64-slice computed tomography angiography of the coronary arteries. *Eur J Radiol* 2006;57:373–9.
13. Wintersperger BJ, Nikolaou K, von Ziegler F, et al. Image quality, motion artifacts, and reconstruction timing of 64-slice coronary computed tomography angiography with 0.33-second rotation speed. *Invest Radiol* 2006;41: 436–42.
14. Pannu HK, Jacobs JE, Lai S, et al. Coronary CT angiography with 64-MDCT: assessment of vessel visibility. *AJR Am J Roentgenol* 2006;187:119–26.
15. Leschka S, Husmann L, Desbiolles LM, et al. Optimal image reconstruction intervals for non-invasive coronary angiography with 64-slice CT. *Eur Radiol* 2006; 16:1964–72.
16. Horiguchi J, Kiguchi M, Fujioka C, et al. Radiation dose, image quality, stenosis measurement, and CT densitometry using ECG-triggered coronary 64-MDCT angiography: a phantom study. *AJR Am J Roentgenol* 2008;190:315–20.
17. Sun Z. Multislice CT angiography in aortic stent grafting: relationship between image noise and body mass index. *Eur J Radiol* 2007;61:534–40.
18. Yoshimura N, Sabir A, Kubo T, et al. Correlation between image noise and body weight in coronary CTA with 16-row MDCT. *Acad Radiol* 2006;13:324–8.
19. Jones CM, Athanasiou T, Dunne N, et al. Multi-slice computed tomography in coronary artery disease. *Eur J Cardiothorac Surg* 2006;30:443–50.
20. Rybicki FJ, Otero HJ, Steigner ML, et al. Initial evaluation of coronary images from 320-detector row computed tomography. *Int J Cardiovasc Imaging* 2008;24:535–46.
21. Ferencik M, Moselewski F, Ropers D, et al. Quantitative parameters of image quality in multidetector spiral computed tomographic coronary imaging with sub-millimeter collimation. *Am J Cardiol* 2003;92:1257–62.
22. Heyer CM, Mohr PS, Lemburg SP, et al. Image quality and radiation exposure at pulmonary CT angiography with 100- or 120-kVp protocol: prospective randomized study. *Radiology* 2007;245:577–83.
23. Cademartiri F, Mollet NR, van der Lugt A, et al. Intravenous contrast material administration at helical 16-detector row CT coronary angiography: effect of iodine concentration on vascular attenuation. *Radiology* 2005;236:661–5.
24. Fleischmann D. Use of high-concentration contrast media in multiple-detector-row CT: principles and rationale. *Eur Radiol* 2003;13(Suppl 5):M14–20.

六十四切面電腦斷層攝影篩檢冠狀動脈影像品質之參數定量分析

楊麗華[1] 吳定國[1,2] 陳巧雲[1,2] 劉金昌[1,2] 謝賜吉[1,2] 趙垂勳[1,2] 黃淑媛[1] 林倩仲[1] 許瑞昇[3,4]

[1]高雄醫學大學附設醫院 影像醫學部

高雄醫學大學 [2]醫學系 [3]醫學研究所

[4]高雄市立小港醫院 影像醫學科

藉由高影像品質準確的診察整體冠狀動脈是決定多層切面電腦斷層冠狀動脈攝影成為臨床上常規應用的關鍵。為了評估六十四切面電腦斷層冠狀動脈的影像品質，本研究回顧以參數定量分析來評估 105 位（ 71 位男性，34 位女性；年齡 58.66 ± 10.62 歲）因為健康檢查以六十四切面電腦斷層冠狀動脈血管攝影來篩檢冠狀動脈疾病的受檢者。結果發現評估者之間在冠狀動脈的半定量影像品質，可見的冠狀動脈長度，訊號－雜訊比與對比－雜訊比的測量有很好的一致性。冠狀動脈近端的訊號－雜訊比與對比－雜訊比優於冠狀動脈遠端（$p < 0.001$）。右冠狀動脈有狹窄者可測量的右冠狀動脈長度比右冠狀動脈沒有狹窄者短（$p = 0.03$）冠狀動脈有狹窄者與沒有狹窄者在冠狀動脈之訊號－雜訊比與對比－雜訊比沒有顯著差異（$p > 0.05$）。體重和身高體重指數與主動脈之訊號－雜訊比和對比－雜訊比呈反比（$p < 0.001$）。雖然冠狀動脈遠端的訊號－雜訊比與對比－雜訊比劣於近端，但是大部分的受檢查的冠狀動脈都有很好的影像品質。因此六十四切面電腦斷層對於建康檢查的受檢者可以提供良好品質的冠狀動脈影像。

關鍵詞：電腦斷層攝影，冠狀動脈

(高雄醫誌 2010;26:21–9)

收文日期：98 年 8 月 20 日

接受刊載：98 年 9 月 9 日

通訊作者：許瑞昇醫師

高雄市立小港醫院影像醫學科

高雄市 812 小港區山明路 482 號